INVESTIGATION OF THE MECHANICAL PROPERTIES OF STANDARD MALAYSIAN RUBBER WITH CONSTANT VISCOSITY AND EPOXIDISED NATURAL RUBBER USING NANO-INDENTATION TEST

Mohd Azli Salim[1,2,*], Adzni Md. Saad[1], Azmi Naroh[3], Mohd Nizam Sudin[1], Crtomir Donik[4], Norbazlan Mohd Yusof[5] & Intan Raihan Asni Rosszainily[1]

[1]Fakulti Kejuruteraan Mekanikal, Universiti Teknikal Malaysia Melaka (UTeM), Malaysia
[2]Advanced Manufacturing Centre, Universiti Teknikal Malaysia Melaka (UTeM), Malaysia
[3]Jabatan Kejuruteraan Mekanikal, Politeknik Ungku Omar, Malaysia
[4]Institute of Metals and Technology, Slovenia
[5]Centre of Excellence, Projek Lebuhraya Usahasama Berhad (PLUS), Malaysia

[*]Email: azli@utem.edu.my

ABSTRACT

The usage of natural rubber (NR) in the development of laminated rubber-metal spring (LR-MS) for automotive applications has led to the investigation on its mechanical properties. This paper describes the use of nano-indentation test to investigate the mechanical properties of standard Malaysian rubber (SMR) with constant viscosity and epoxidised natural rubber (ENR). The mechanical properties of SMR Constant Viscosity 60 (SMR CV-60) and 25 mole % ENR (ENR 25) reinforced with 0, 20, 40 and 60 phr of carbon black (CB) was investigated. The nano-indentation test was carried out using Berkovich tips at constant load of 2 mN with holding times of 0, 5, 10, 15, and 20 s. It was found that the SMR CV-60 and ENR 25 compounds with 60 phr CB loading recorded the highest hardness and elastic modulus values, and also had the lowest penetration depth. The test also revealed that the hardness and penetration depth were independent to the holding times. In contrast, the indentation elastic modulus was found to be highly affected by the holding time.

Keywords: *Standard Malaysian rubber (SMR); natural rubber (NR); epoxidised natural rubber (ENR); nano-indentation.*

1. INTRODUCTION

Rubbers are available in two types, which are synthetic and natural. Synthetic rubber is an artificial rubber that is produced through the polymerisation process of petroleum by-product. It was invented to reduce dependencies on the natural rubber (NR) during the World War II. As for today, there are more than 20 types of synthetic rubber that are available for various applications. On the other hand, NR is naturally extracted from rubber trees through the tapping process, which is a process of latex secretion by shearing a thin layer of rubber tree's bark by using a special tapping knife. There are more than 2,500 known species of plants that can produce latex. In spite of that, only latex produced from the *Hevea Brasiliensis* tree is mostly used for rubbery products due to its quality (Lindley, 1964; Aravind *et al*., 2015).

Although synthetic rubbers are well known to offer numerous advantages in terms of mechanical and chemical properties, NR also possesses advantages over synthetic rubbers. NR can be considered as green material since it can be continuously supplied by nature as compared to the synthetic rubber, which is derived from the non-renewable sources (Boonkerd, 2017). Besides that, the price of raw NR is more economical than synthetic rubber. The price of synthetic rubber normally fluctuates depending on the current crude oil prices. Other than that, the properties of NR compounds can be derived from better formulation and processing. NR also allows low heat build-up in dynamic force to

make it able to withstand large deformations and grants it with the ability to instantly recover when distorted at room temperature (Chandrasekaran, 2010). The application of NR as the main material for vibration isolator in automotive applications does not require extensive maintenance due to its capability of maintaining itself for a long period of time. Additionally, NR also exhibits inherent damping and spring-like performance in order to reduce the resonance effect. NR can be bonded with other materials such as metal in order to increase its strength (Heide *et al*., 2018).

As one of the largest NR manufacturers and exporters, Malaysia has taken an initiative to promote local NR in various fields, including construction, automotive and sports. The Malaysian government has established the Malaysian Rubber Board (MRB) and Tun Abdul Razak Research Centre (TARRC) to provide the best infrastructure for research and development of local NR. The quality and competitiveness of Malaysian NR products, especially in vibration isolation, has been proven as one of the best in the world. One of the examples of Malaysian NR applications in vibration isolation can be found in the structure of the Sultan Abdul Halim Muadzam Shah Bridge, Penang that is equipped with high damping NR to withstand from possible large earthquakes (Picken *et al*., 2012). Besides that, most of the Malaysian ports also use the Malaysian-made dock fenders as a bumper to absorb impact from collisions between boats and jetties (Yu *et al*., 2001; Kim *et al*., 2004).

Based on previous research, it was found that the development of the laminated rubber-metal spring (LR-MS) for automotive mounting applications is currently in trend (Salim *et al*., 2013, 2014, 2016). The study on the transmissibility in the axial direction and parameter assessment on LR-MS was conducted. This study looks into the application of Malaysian NR, which is the vulcanised standard Malaysian rubber constant viscosity 60 (SMR CV-60) reinforced with carbon black (CB) as the potential main material, combined with a metal plate for the development of LR-MS. In order to determine the compatibility of local NR grade as the main substance in the development of LR-MS, the mechanical properties of rubber reinforced with CB need to be investigated.

This study focuses on the investigation of the mechanical properties of vulcanised SMR CV-60, reinforced with different CB loadings ranging from 0, 20, 40 and 60 part per hundred of rubber (phr) using nano-indentation test. Besides that, the commercial 25% mol ENR (ENR 25) with similar compounding formula and CB loading was also used as a comparison to SMR CV-60. Nano-indentation test is used in this study as it is more cost-effective and non-destructive, as well as requiring smaller test pieces as compared to conventional techniques.

2. METHODOLOGY

This section describes in detail the methodologies for material preparation and nano-indentation test.

2.1 Material Preparation

Two types of NR compound were used in this study, namely vulcanised SMR CV-60 and vulcanised ENR 25. As a collaboration with the Malaysian Rubber Board (MRB), the material preparation of milling and mixing, as well as the vulcanising processes were conducted in MRB's accreditation laboratory in order to maintain the quality of the compounded rubber.

The composition ingredients for the rubber compound were prepared based on phr. The complete formulation for both rubbers is tabulated in Table 1. The addition of sulphur helped to increase the crosslinking in the rubbers, which resulted in the improvement of rubber texture from soft to hard. Meanwhile, the other ingredients, such as zinc oxide, stearic acid and N-cyclohexyl benzothiazyl sulphenamide (CBS), worked as the accelerator to boost up the sulphur crosslink efficiency. Santoflex 13 and paraffin wax were also added into the compound as ozone protective agents. N330 CB was used as the filler due to its good surface activity and chemical properties, which influenced good

interface interaction between the rubber chain and CB particles (Sangwichien *et al*., 2008). In this study, the CB loading in the NR compounds was set as the changing parameter, which varied at 0, 20, 40 and 60 phr.

Table 1: Formulation for the SMR CV-60 and ENR 25 compounds.

Ingredient	Amount (phr)
SMR CV-60/ ENR 25	100
Zinc Oxide	5
Stearic Acid	2
CBS	0.8
Sulphur	3.25
Black HAF, N330	0, 20, 40, 60
Santoflex 13	3
Parafin Wax	2

The equipment specifications and procedures for the mixing and vulcanisation processes were based on ASTM D3182: Standard Practice for Rubber-Materials, Equipment, and Procedures for Mixing Standard Compounds and Preparing Standard Vulcanized Sheets, which is the guideline for preparing standard vulcanised rubber sheets. The compounding process was started by mixing the dried NR with other ingredients in the rolling machine for about 10 to 15 min. Then, the compound was left to rest for at least 4 h to reach its steady state before moving to the next process. The rheometer test was conducted on the compound in order to obtain the parameter for the vulcanisation process. The compounds were vulcanised at temperature of 150 ˚C for 8 to 12 min, depending on the CB compositions in the NR compound. The vulcanising process refers to the treating of rubber materials with sulphur in the presence of great heat to improve its elasticity and hardness.

2.2 Test Load Determination

This study provides the findings of conducting the nanoindentation test on vulcanised natural rubber compounds of SMR CV-6 and ENR 25. An indentation-creep test was conducted at various holding times starting from 0 to 20 s. A fixed 2 mN test force was used as the maximum peak load. As there was no specific peak load stated in the ASTM standard, the peak load value was determined by referring to Oyen (2007) as a precaution in order to avoid excessive applied force or the indenter tip to indent over the specimen.

Oyen (2007) determined the peak load level (P_{max}) range, depending on the material's elastic modulus ($E_{elastic}$) and Poisson's ratio (υ). This researcher applied P_{max} ranging from 1 mN and 10 mN to indent materials with $E_{elastic}$ = 210 MPa and 4 MPa with υ = 0.42 and 0.50 respectively. The researcher used a spherical tip to indent up to 3.05 mm from the thickness of the material. By referring to the range of P_{max} as stated in the previous research as the limit for maximum applied force and the Young's Modulus value obtained from the tensile and compression tests, 2 mN test force was used in this study.

2.3 Nano-Indentation Setup

The indentation test was used to determine the strength properties of material through its surface. In this study, the nano-indentation test was conducted to measure the specimens Young's Modulus and other properties. The effects of holding time on the material properties was also investigated. The experiment was conducted by referring to the ASTM standard E2546-15: Standard Practice for Instrumented Indentation Testing. This standard only covers the practice requirement of indentation testing without specifying any test force, indentation depth range or any specific indenter types.

All the tests were performed at ambient temperature of 23 ˚C. The indentation test was conducted on eight samples with four different CB loadings using a nano-hardness tester (Shimadzu Dynamic Ultra Micro Hardness Tester Model DUH-211). The nano-indenter device was equipped with an imaging device that is capable to switch back and forth from the optical microscope to the indenter tips. The mounted imaging device helps to accurately identify the desirable indentation point. A standard Berkovich type 115˚ triangular pyramidal indenter was used in this study. The machine was operated with the aid of the DUH211 software that comes together with the equipment.

Both vulcanised rubber sheets with 2 mm thickness were cut into 10 mm x 10 mm squares for the tests. The test piece size was determined by referring E2546-15. The test piece thickness was set to be at least 10 times of the maximum indentation depth (if conducting displacement assessment) or six times of the indentation radius. Meanwhile, the test piece size should not be too small or too big, depending on the size of indenter holder. All the test pieces' surfaces were wiped off with a damp cloth to remove dirt that might affect the indentation results. The test pieces were let to completely dry before testing.

Each test piece was mounted on a platform to keep it stationary while conducting the indentation test. The test piece was placed under an optical microscope to determine the indentation point before the platform was moved to the indenter side. The load-hold-unload test was conducted with a fixed maximum test force of 2 mN and constant indenter loading speed of 0.2926 mN/sec. The maximum test force was determined by considering certain conditions, such as the test piece thickness, types of materials, probability of materials to deform during indentation, surface finish, and machine competency. The indentation tests were also conducted at different holding times, which varied from 0, 5, 10, 15, and 20 s. All the tests were conducted with three repetitions, where the mean and standard deviation were calculated using Equations 1 and 2 respectively.

$$\bar{x} = \frac{\sum fx}{n} \tag{1}$$

and

$$S = \sqrt{\frac{\sum \left(x - \bar{x} \right)^2}{n-1}} \tag{2}$$

where $\bar{x}$ is the mean values of the data set, n is the number of data set, and $\sum fx$ is the summation of the all the data set. S represents the standard deviation of the sample, $\sum$ means "sum of", and x represent each value in the dataset.

This study was carried out with two assumptions: no sink-in and pile-up effect were accounted during the experiment. The nano-indentation results were recorded and presented in terms of maximum force (F_{max}), maximum indentation depth (h_{max}), hardness (H_u), and Elastic Modulus (E_{it}).

3. RESULTS & DISCUSSION

3.1 Effect of CB Loading

The experimental results for the nano-indentation test on SMR CV-60 and ENR 25 filled with CB loadings of 0, 20, 40 and 60 phr are shown in Tables 2 and 3. Based on the obtained results, the recorded maximum force ranged from 2.00 to 2.01 MPa in response to the test constant parameter, which was the maximum indentation load at 2 mN.

Table 2: The nano-indentation properties for the SMR CV-60 compounds.

Nano-indentation properties	Carbon loading (phr)			
	0	20	40	60
Maximum Force (F_{max}, mN)	2.01±0.01	2.01±0.01	2.00±0.01	2.01±0.01
Maximum Indentation Depth ($h_{max,}$ μm)	15.36±1.00	13.13±0.25	9.25±1.00	7.20±0.87
Hardness (H_u , MPa)	0.33±0.04	0.44±0.02	0.91±0.21	1.80±0.41
Elastic Modulus (E_{it} , MPa)	5.01±0.79	7.21±0.23	18.29±4.27	42.51±4.27

Table 3: The nano-indentation properties for the ENR 25 compounds.

Nano-indentation properties	Carbon loading (phr)			
	0	20	40	60
Maximum Force (F_{max}, mN)	2.01±0.01	2.00±0.01	2.02±0.01	2.01±0.01
Maximum Indentation Depth ($h_{max,}$ μm)	12.89±0.45	12.47±1.09	8.69±0.87	6.65±1.54
Hardness (H_u , MPa)	0.44±0.03	0.50±0.09	1.03±0.22	1.42±1.04
Elastic Modulus (E_{it} , MPa)	7.21±1.61	8.57±2.12	21.17±2.71	51.26±18.84

The relationship between h_{max} and the CB loading of SMR CV-60 and ENR 25 is presented in Figure 1. It shows that the h_{max} values decreased with the increase of CB loadings for both NR compounds. Besides that, the h_{max} value for SMR CV-60 was slightly higher as compared to ENR 25. The highest h_{max} value recorded by SMR CV-60 was 15.36 μm, while the lowest was 7.20 μm. Meanwhile, the highest h_{max} value for the ENR 25 compounds was 12.89 μm, while the lowest was 6.65 μm.

The graph of H_u versus CB loadings is presented in Figure 2. Both NR compounds exhibited similar graph trend, where H_u was found to increase as the CB loadings was increased. Additionally, the graph also showed that the H_u value of SMR CV-60 was slightly lower than ENR 25 with the CB loadings of 0 phr to 40 phr and conversely higher at 60 phr. The H_u values at 0 phr were 0.33 MPa for SMR CV-60 and 0.46 MPa for ENR 25. H_u increased slightly at 20 phr with the value of 0.44 MPa for SMR CV-60 and 0.50 MPa for ENR 25. Then, at 40 phr, the H_u value was found to gradually increase at the value of 0.91 MPa for SMR CV-60 and 1.03 MPa for ENR 25. The H_u values for SMR CV-60 and ENR 25 at 60 phr were 1.80 and 1.42 MPa respectively.

The correlation between h_{max} and H_u can be found in Figures 1 and 2, where h_{max} was found to decrease while H_u increased with the increase of CB loadings. This is as the increase of CB loadings increased the hardness of NR, thus enhancing the NR stiffness to become less elastic. This restrained the indenter tips to penetrate further into the materials, resulting in lower h_{max} as the compound contains high CB loadings (Callister & Rethwisch, 2011).

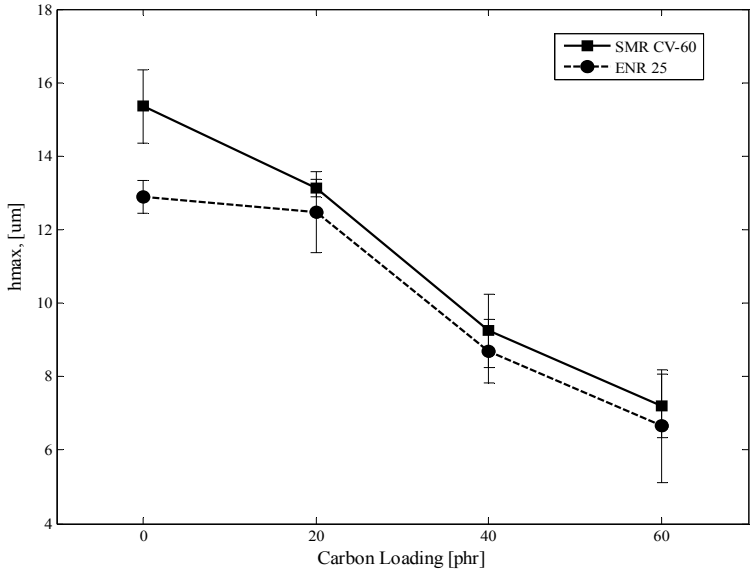

Figure 1: The graph of maximum indentation depth (h_{max}) versus CB loadings for SMR CV-60 and ENR 25.

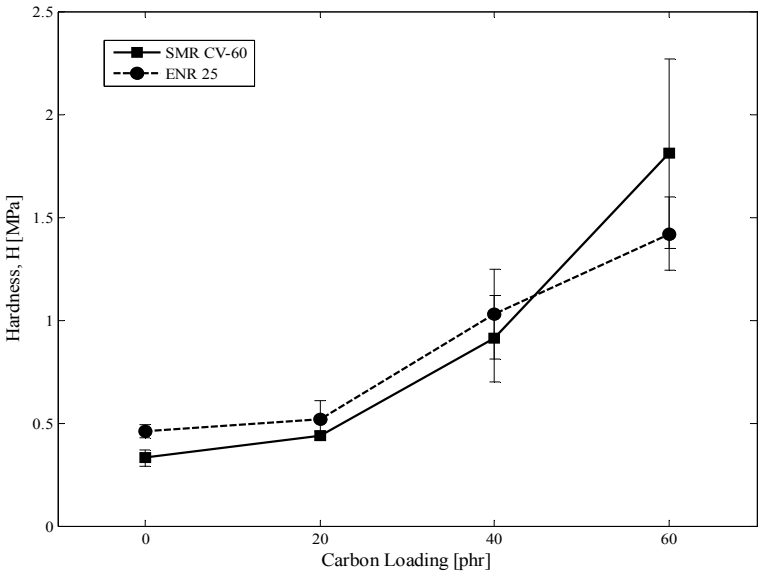

Figure 2: The graph of hardness (H_u) versus the CB loadings for SMR CV-60 and the ENR 25.

The graph of E_{it} for SMR CV-60 and ENR 25 at different CB loadings is depicted in Figure 3. It is found that E_{it} for SMR CV-60 was slightly increased from 0 to 20 phr of CB loadings. Contrarily, E_{it} for ENR 25 was found to slightly decrease from 0 to 20 phr. Subsequently, the E_{it} values for both NR compounds were found to exhibit a significant increment as the CB loadings was increased up to 60 phr. The recorded E_{it} values for SMR CV-60 were 5.01, 7.21, 18.29, and 42.51 MPa at 0, 20, 40 and 60 phr of CB loadings respectively. On the other hand, the recorded values for ENR 25 were 8.58, 8.57, 21.17 and 51.26 MPa at 0, 20, 40 and 60 phr of CB loadings respectively. The graph also showed that the E_{it} values of the ENR 25 compounds were higher as compared to the SMR CV-60 compounds. This shows that the CB particles interact better with the ENR 25 particles to produce stronger NR chains as compared to the SMR CV-60 particles.

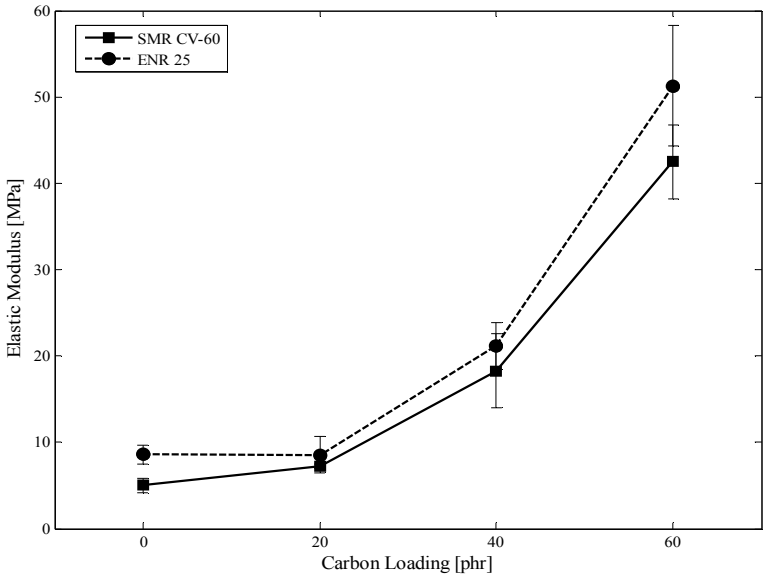

Figure 3: The graph of elastic modulus (E_{it}) versus the CB loadings for the SMR CV-60 and the ENR 25.

3.2 Effect of Different Holding Times

In this study, both compounds with different CB loading was indented at holding times of 5, 10, 15, and 20 s, with the results presented accordingly in Table 4 and Table 5. Based on the table, it was found that h_{max} varied at different holding time. This is due to the adhesion in rubbery materials. In compared to metals, the NR possesses a soft and tacky surface that will be attracted to the indenter tips during preloading, resulting in negative load and displacement values at the beginning of test (Chandrashekar *et al*., 2015).

Table 4: The nano-indentation properties of SMR CV-60 at different holding times.

Time (s)	Nano-indentation properties	Carbon loading (phr)			
		0	20	40	60
5	Maximum Force (F_{max}, mN)	1.97±0.03	1.97±0.03	2.00±0.03	2.01±0.02
	Maximum Indentation Depth ($h_{max,}$ μm)	16.55±0.19	13.65±0.56	10.08±1.51	6.22±0.56
	Hardness (H_u , MPa)	0.28±0.01	0.41±0.03	0.78±0.21	2.36±0.94
	Elastic Modulus (E_{it} , MPa)	4.15±0.10	6.87±0.43	14.55±2.93	45.47±3.06
10	Maximum Force (F_{max}, mN)	1.99±0.02	1.99±0.00	1.99±0.00	2.01±0.02
	Maximum Indentation Depth ($h_{max,}$ μm)	18.14±1.18	13.30±0.27	9.85±2.21	6.68±0.28
	Hardness (H_u , MPa)	0.23±0.03	0.43±0.02	0.88±0.21	1.71±0.94
	Elastic Modulus (E_{it} , MPa)	3.61±0.38	7.85±0.22	16.15±6.43	48.93±1.34
15	Maximum Force (F_{max}, mN)	1.98±0.01	1.99±0.00	1.99±0.00	2.00±0.01
	Maximum Indentation Depth ($h_{max,}$ μm)	19.28±1.10	13.50±0.55	10.10±1.20	5.34±0.79
	Hardness (H_u , MPa)	0.20±0.02	0.42±0.03	0.80±0.20	2.23±0.65
	Elastic Modulus (E_{it} , MPa)	3.09±0.31	7.90±0.38	15.12±3.87	56.16±2.04
20	Maximum Force (F_{max}, mN)	1.98±0.02	1.99±0.02	1.99±0.02	2.00±0.01
	Maximum Indentation Depth ($h_{max,}$ μm)	18.90±0.57	12.47±1.10	9.15±1.28	6.13±0.57
	Hardness (H_u , MPa)	0.21±0.01	0.49±0.09	1.02±0.29	2.06±0.42
	Elastic Modulus (E_{it} , MPa)	3.21±0.17	9.08±1.16	18.17±3.98	55.21±3.81

Table 5: The nano-indentation properties of ENR 25 at different holding times.

Time (s)	Nano-indentation properties	Carbon loading (phr)			
		0	20	40	60
5	Maximum Force (F_{max}, mN)	1.99±0.03	1.99±0.02	1.99±0.02	1.99±0.02
	Maximum Indentation Depth ($h_{max,}$ μm)	15.71±0.91	11.51±0.65	8.86±1.14	5.39±0.77
	Hardness (H_u , MPa)	0.31±0.04	0.57±0.07	1.00±0.27	2.71±0.70
	Elastic Modulus (E_{it} , MPa)	5.48±0.71	9.64±0.29	19.18±3.07	54.00±3.68
10	Maximum Force (F_{max}, mN)	1.99±0.03	1.99±0.02	1.98±0.03	1.99±0.03
	Maximum Indentation Depth ($h_{max,}$ μm)	13.89±1.13	11.02±1.06	8.75±0.64	7.38±0.95
	Hardness (H_u , MPa)	0.40±0.06	0.63±0.13	1.00±0.14	1.43±0.36
	Elastic Modulus (E_{it} , MPa)	7.22±1.05	11.67±2.56	21.56±2.59	46.68±7.29
15	Maximum Force (F_{max}, mN)	1.98±0.04	1.98±0.03	1.98±0.03	1.99±0.02
	Maximum Indentation Depth ($h_{max,}$ μm)	15.35±1.12	12.56±1.50	8.89±1.24	5.80±0.66
	Hardness (H_u , MPa)	0.32±0.05	0.47±0.12	0.98±0.25	2.30±0.54
	Elastic Modulus (E_{it} , MPa)	5.88±0.89	8.51±2.57	21.97±4.50	66.74±4.56
20	Maximum Force (F_{max}, mN)	2.00±0.01	2.00±0.01	1.99±0.01	2.00±0.00
	Maximum Indentation Depth ($h_{max,}$ μm)	15.53±0.57	12.92±1.32	8.27±0.42	5.50±0.69
	Hardness (H_u , MPa)	0.34±0.08	0.46±0.09	1.11±0.11	2.58±0.64
	Elastic Modulus (E_{it} , MPa)	6.67±1.07	8.34±1.36	26.17±1.95	84.56±5.29

The relationship between H_u and the different holding times are presented in Figures 4 and 5 for the SMR CV 60 and ENR 25 compounds respectively. Based on the figures, it is found that the H_u values increased as the CB content was increased. However, it is also observed that the H_u values varies with the increase of holding time for both compounds at different CB loadings.

Figure 4 shows that the H_u values of SMR CV-60 with 0 phr of CB loading, was slightly decreased with the increase of holding time. The values ranged from 0.28 MPa to 0.21 MPa. For SMR CV-60 with 20 phr of CB loading, the H_u values fluctuated slightly from 0.41 to 0.49 MPa. The fluctuation differences increased as the CB loading increased. For SMR CV-60 with 40 phr of CB loading, the H_u values ranged from 0.78 to 1.02 MPa, while for SMR CV-60 with 60 phr of CB loading, the H_u values ranged from 1.71 to 2.36 MPa.

As shown in Figure 5, fluctuating trends for H_u were also observed for the ENR 25 compounds with different CB loadings. For ENR 25 with 0 phr of CB loading, the H_u values ranged for 0.31 to 0.40 MPa, while for ENR 25 with 20, 40 and 60 phr of CB loadings, the H_u values ranged from 0.47 to 0.63 MPa, 0.98 to 1.11 MPa, and 1.43 to 2.71 MPa respectively.

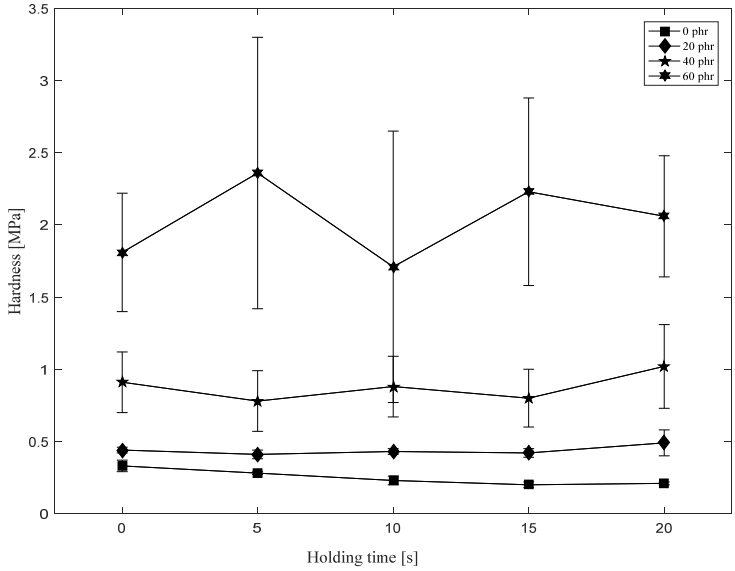

Figure 4: The graph of hardness (H_u) versus the holding time for SMR CV-60.

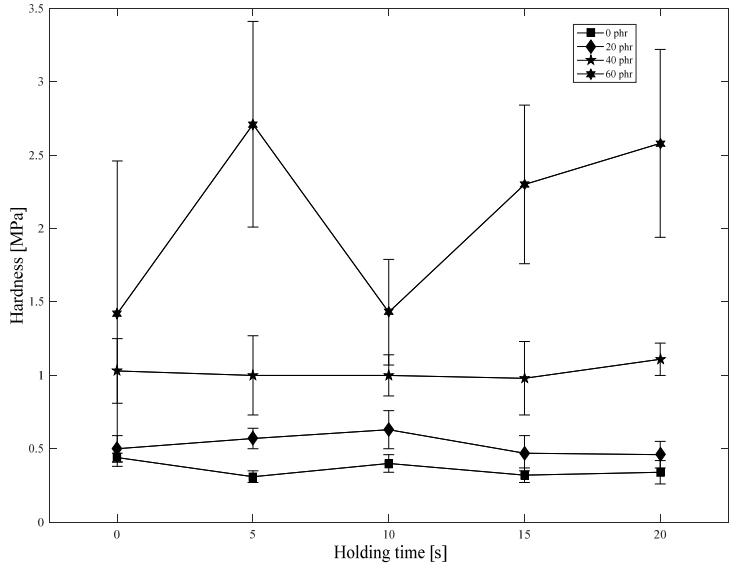

Figure 5: The graph of hardness (H_u)versus the holding time for ENR 25.

The recorded E_{it} values at different holding times were plotted separately in Figures 6 and 7 for SMR CV-60 and ENR 25 at different CB loadings respectively. The E_{it} values for SMR CV-60 at 0 phr CB loading were found to decrease slightly from 5.01 to 3.21 MPa as the holding time increased. In contrast, for SMR CV-60 with the other CB loadings, the E_{it} values were found to increase with the increasing holding time. The E_{it} values for SMR CV-60 with 20 phr CB loading increased slightly from 7.21 to 9.09 MPa. On the other hand, SMR CV-60 with 40 phr and 60 phr CB loadings showed a fluctuating trend for E_{it} as the holding time increased. The E_{it} values for SMR CV-60 with 40 phr CB loading ranged from 14.55 to 18.29MPa, for SMR CV-60 with 60 phr CB loading, it ranged from 42.51 to 56.16 MPa.

The fluctuating trend was also observed for the recorded E_{it} values at different holding times for ENR 25 at different CB loadings. The recorded E_{it} values for ENR 25 showed slight change at various holding times with the range of 5.48 to 8.58 MPa for 0 phr CB loading and 8.33 MPa to 11.67 MPa for 20 phr CB loading. The graph also showed that the E_{it} values for ENR 25 with 40 phr CB loading was significantly higher than ENR 25 with 20 phr CB loading, with the values ranging from 19.18 to 26.17 MPa. As compared to SMR CV-60, ENR 25 with 60 phr CB loading showed a sudden increase in the E_{it} values from 46.68 MPa at 10 s to 66.74 and 84.86 MPa at 15 and 20 s respectively.

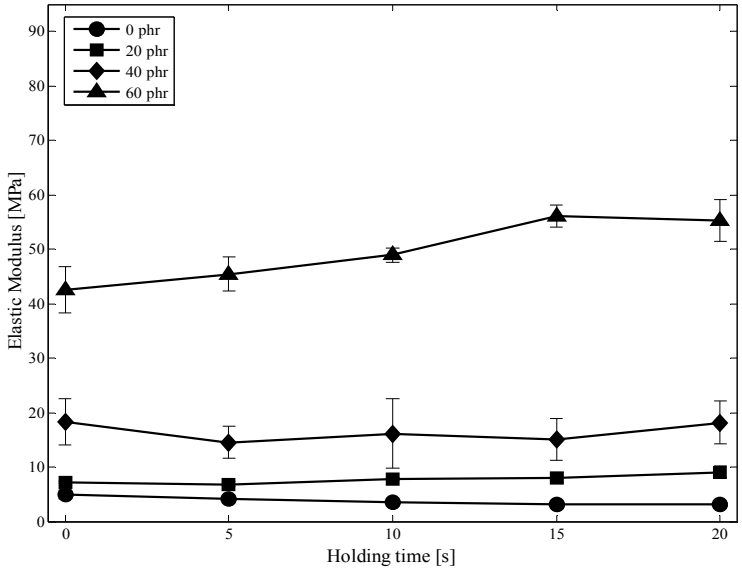

Figure 6: The graph of elastic modulus versus the holding time for SMR CV-60 at different CB loadings.

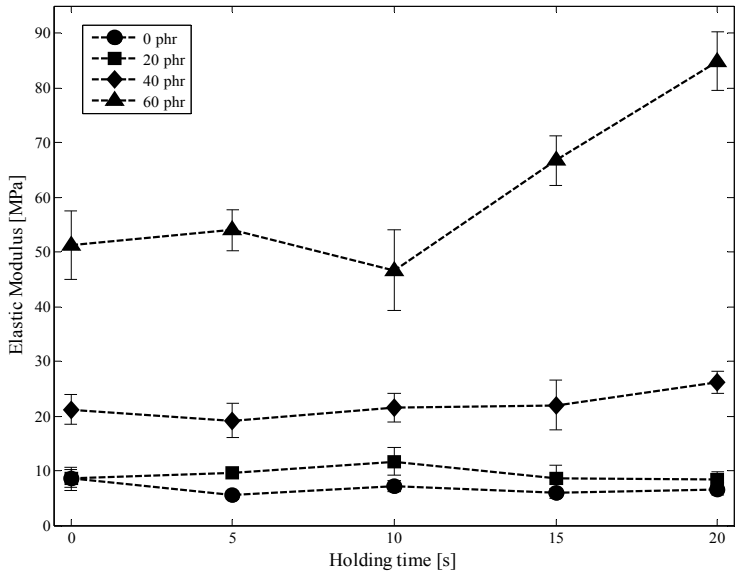

Figure 7: The graph of elastic modulus versus the holding time for ENR 25 at different CB loadings.

Figures 6 and Figure 7 show that the E_{it} values are slightly dependent on the holding time for both NR compounds at 0, 20 and 40 phr CB loadings. In contrast, significant changes were observed the compounds with high CB content (60 phr), where the E_{it} values were found to increase with increasing holding time. As in nano-indentation, the holding time was applied to minimise the creep effect on the unloading curve, which may affect the hardness and elastic modulus reading. The holding time also highly affects the E_{it} for some materials that are indented by the Berkovich tip (Han *et al*., 2016).

Additionally, the fluctuating E_{it} values observed for SMR CV-60 and ENR 25 with lower CB content were caused by experimental uncertainties that affecting the nano-indentation test results, such as machine compliance, thermal drift and NR surface roughness. The standard deviation bar showed in each graph represents the variation of values in the collected data, which was caused by the experimental uncertainties that could directly affect the instrument performance and indentation results. The instrument or machine compliance for calibration of the initial contact between the sample and mounted tips, as well as imprecise machine stiffness value could significantly affect the measured indentation force and penetration depth data. Besides that, the effect of thermal drift, which occurs due to the machine thermal expansion and heat generated by continuously running the

electronic device is quite significant on soft polymer, especially when indented at lower maximum depth and time relaxation (Lin *et al*., 2007; Chandrashekar *et al*., 2015).

3.3 Indentation Work Dissipation

The results for the work dissipation coefficient (μ_{in}) in the indentation of SMR CV-60 and ENR 25 at different CB loadings under different holding times are presented in Tables 6 and 7. μ_{in} can be described as the ratio of indentation work value for the elastic component to the total indentation work (W_{total}). W_{total} is the total of elastic and inelastic work components, which is expressed as in Equation 3.

$$W_{total} = W_{in}^{elastic} + W_{in}^{inelastic} \tag{3}$$

The dissipated work depends not only on H_u and E_{it}, but also on the elastic recovery of material during the unloading process (Recco *et al*., 2009). Based on the tables, at 0 s holding time, the μ_{in} values decreased as the CB loading increased. Besides that, both compounds showed similar behaviour, where fluctuating μ_{in} values were found, except for SMR CV6 with 20 phr CB loading, whereby μ_{in} decreased with increasing holding time. It was also found that the μ_{in} values for SMR CV60 were higher than ENR 25 with similar CB loadings. This behaviour shows the irreversibility of plastic deformation of both rubber compounds and its capability to store elastic energy at different CB loadings and holding times.

Table 6: Work dissipation coefficient (μ_{in}) for SMR CV-60 at different holding times.

Work dissipation coefficient (μ_{in} ,%)						
Carbon loading (phr)		Holding time (s)				
		0	5	10	15	20
SMR CV-60	0	66.77	66.74	59.51	61.26	60.90
	20	58.48	54.78	49.32	47.35	47.29
	40	47.60	47.86	49.93	47.51	45.32
	60	34.98	31.99	28.27	27.64	34.32

Table 7: Work dissipation coefficient (μ_{in}) of ENR 25 at different holding times.

Work dissipation coefficient (μ_{in} ,%)						
Carbon loading (phr)		Holding time (s)				
		0	5	10	15	20
ENR 25	0	52.02	50.17	41.26	45.24	48.56
	20	47.12	38.35	36.20	44.94	43.64
	40	43.67	39.28	36.19	30.69	31.72
	60	29.60	28.93	24.72	24.00	24.43

4. CONCLUSION

The results of the nano-indentation test conducted in this study shows that the properties of the SMR CV60 and ENR 25 compounds were highly affected by the CB loadings. The indentation depth decreased as the CB loadings in the SMR CV-60 and ENR 25 compounds were increased. This shows that the increasing CB loading increased the stiffness of the NR compounds, thus increasing the resistance of the NR compounds from indenter tip penetration. In addition, the hardness and elastic modulus values also increased with the increasing CB loading for both NR compounds. Meanwhile, in the investigation of the effect of holding time on the indentation of the Berkovich tips, it showed that the indentation properties were slightly dependent on the holding time, whereby the penetration depth, hardness and elastic modulus values fluctuated as the holding time increased. The dependency

of holding time was clearest for the SMR CV-60 and ENR 25 compounds with 60 phr CB loading. The work dissipation coefficient study also showed that the capability of both compounds to store elastic energy is highly depended on the CB loadings and holding times.

ACKNOWLEDGEMENTS

The authors are grateful to the Advanced Manufacturing Centre and Fakulti Kejuruteraan Mekanikal, Universiti Teknikal Malaysia Melaka (UTeM) for providing the laboratory facilities used in this study.

REFERENCES

Ab-Malek, K., Ahmadi, H.R., Muhr, A.H., Stephens, I.J., Gough, J., Picken, J.K. & Taib, I.M. (2012). Seismic protection of 2nd Penang crossing using high damping natural rubber isolators. *15th World Conf. Earthquake Eng.,* Lisbon.

Aravind, A., Joy, M. L., & Nair, K. P. (2015). Lubricant properties of biodegradable rubber tree seed (Hevea brasiliensis Muell. Arg) oil. *Ind. Crop. Prod.*, **74**: 14-19. ASTM, D. 3182. (2016). *Standard Practice for Rubber—Materials, Equipment, and Procedures for Mixing Standard Compounds and Preparing Standard Vulcanized Sheets*. Annual Book of ASTM standards. ASTM International, West Conshohocken, Pennsylvania.

ASTM, E. 2546. (2015). *Standard Practice for Instrumented Indentation Testing*. Annual Book of ASTM Standards. ASTM International, West Conshohocken, Pennsylvania.

Atrian, A., Majzoobi, G. H., Nourbakhsh, S. H., Galehdari, S. A. & Nejad, R. M. (2016). Evaluation of tensile strength of Al7075-SiC nanocomposite compacted by gas gun using spherical indentation test and neural networks. *Adv. Powder Technol*, **27**: 1821-1827.

Boonkerd, K. (2017). Development and modification of natural rubber for advanced application. In *Applied Environmental Materials Science for Sustainability*. IGI Global, Pennsylvania, pp. 44-76.

Callister, W.D. & Rethwisch, D.G. (2011). *Materials Science and Engineering: An Introduction*. Wiley, New York.

Chandrashekar, G., Alisafaei, F. & Han, C.S. (2015). Length scale dependent deformation in natural rubber. *J Poly. Sci.*, **132**: 42683

Han, C. S., Sanei, S. H., & Alisafaei, F. (2016). On the origin of indentation size effects and depth dependent mechanical properties of elastic polymers. *J. Polym. Eng.*, **36**: 103-111.

Heide-Jørgensen, S., Møller, R.K., Buhl, K.B., Pedersen, S.U., Daasbjerg, K., Hinge, M. & Budzik, M.K., (2018). Efficient bonding of ethylene-propylene-diene M-class rubber to stainless steel using polymer brushes as a nanoscale adhesive. *Int. J. Adhes. Adhes*, **87**: 31-41.

Kim, W.D., Lee, H.J., Kim, J.Y., & Koh, S.K. (2004). Fatigue life estimation of an engine rubber mount. *Int. J. Fatigue*, **26**: 553-560.

Lin, D.C., Dimitriadis, E.K. & Horkay, F. (2007). Elasticity of rubber-like materials measured by AFM nano-indentation. *Express Polym. Lett.*, **1**: 576-584.

Lindley, P.B. (1964). *Engineering Design with Natural Rubber*. Malayan Rubber Board, Malaysia.

Oliver, W.C. & Pharr, G.M. (1992). An improved technique for determining hardness and elastic modulus using load and displacement sensing indentation experiments. *J. Mater. Res.*, **7**: 1564-1583.

Oyen, M.L. (2007). Sensitivity of polymer nanoindentation creep measurements to experimental variables. *Acta Mater.*, **55**: 3633-3639.

Recco, A.A.C., Viáfara, C.C., Sinatora, A. & Tschiptschin, A.P. (2009). Energy dissipation in depth-sensing indentation as a characteristic of the nanoscratch behavior of coatings. *Wear*, **267**: 1146-1152.

Salim, M. A., Putra, A., & Abdullah, M. A. (2014). Analysis of axial vibration in the laminated rubber-metal spring. *Adv Mater Res.,* **845**: 46-50.

Salim, M. A., Putra, A., Mansor, M.R., Musthafah, M.T., Akop, M.Z. & Abdullah, M.A. (2016). Analysis of parameters assessment on laminated rubber-metal spring for structural vibration. *IOP Conf Ser. Mater. Sci. Eng.*, **(Vol. 114**: 012014.

Salim, M. A., Putra, A., Thompson, D., Ahmad, N. & Abdullah, M.A. (2013). Transmissibility of a laminated rubber-metal spring: A preliminary study. *Appl. Mech. Mater.*, **393**: 661-665.

Sangwichien, C., Sumanatrakool, P. & Patarapaiboolchai, O. (2008). Effect of filler loading on curing characteristics and mechanical properties of thermoplastic vulcanizate. *Chiang Mai J.Sci.*, **35**:141–149.

Thomas, S. & Stephen, R. (Eds.). (2010). *Rubber Nanocomposites: Preparation, Properties, and Applications*. John Wiley & Sons, Singapore.

Xu, F., Ding, Y.H., Deng, X.H., Zhang, P. & Long, Z L. (2014). Indentation size effects in the nano- and micro-hardness of a Fe-based bulk metallic glass. *Physica B: Condensed Matter*, **450**: 84-89.

Yu, Y., Naganathan, N.G., & Dukkipati, R.V. (2001). A literature review of automotive vehicle engine mounting systems. *Mech Mach Theory*, **36**: 123-142.